Electrophoretic and Structural Studies of DNA-directed Au Nanoparticle Groupings

Daniela Zanchet[S], Christine M. Micheel, Wolfgang J. Parak, Daniele Gerion, Shara C. Williams, A. Paul Alivisatos*

Department of Chemistry, University of California, Berkeley

Materials Science Division, Lawrence Berkeley National Laboratory

[S]Present address: Laboratório Nacional de Luz Síncrotron, Cx.P. 6192, Campinas, SP, BRAZIL

* To whom correspondence should be addressed.

UCB – Chemistry Dept.

Berkeley-CA 94720-1460 USA

alivis@uclink4.berkeley.edu

Abstract

Discrete Au nanoparticle/DNA conjugates have been isolated by electrophoresis and used to form small groupings of particles, such as dimers and trimers. The use of purified conjugates leads to a higher yield of the target structure, and it has allowed us better control and understanding of the system. Newly accessible questions, such as the electrophoretic mobility of nanoparticle/DNA hybrids and the critical role of particle surface charge on mobility have been studied. Detailed characterization by Transmission Electron Microscopy (TEM) has now been done due to the higher quality of the samples. A computer program to generate pair distribution functions from TEM images was developed, pointing out the dependence of interparticle distance with DNA length on dimers of particles.

Introduction

The overlap between molecular biology and nanoscience has created a wide array of exciting new possibilities for research and technological applications [1,2]. One vein of this research centers on the use of nanoparticles to address issues of interest to biology. Nanoparticles possess properties—optical, electrical, or magnetic, for example—that can be used to probe biological systems in ways not accessible to traditional biological methods. Examples of this kind of application include the successful use of semiconductor nanocrystals in multi-color cell and DNA labeling [3-10]. Another application is the development of sensitive DNA mismatch detection using metal nanoparticles [11,12]. Also, DNA arrays have been used to sort multiple colors of fluorescent nanocrystals, indicating the potential for nanocrystal use in applications such as gene mapping and microarray analysis [9].

Another important avenue for research at the boundary between nanoscience and molecular biology is the use of biological molecules to address issues of interest to nanoscience. For example, biomolecules have been used to tailor particle properties, such as size control: it has been shown that extensive selection of peptides can lead to species that bind preferentially to specific crystallographic faces of semiconductors; this has been explored to induce the growth of nanoparticles with different crystallographic structures [13]. Also, the recognition properties of biomolecules have been harnessed for the creation of several kinds of nanostructures [14-20]. Both aggregate materials and discrete "nanocrystal molecules" have been synthesized.

In this area, our work has centered on the creation of discrete groupings of Au nanoparticles connected with DNA. There are several advantages to this approach. First, the structures created are discrete: the structure resulting from a given set of starting materials is predictable and can be reproduced precisely and accurately. In addition, it is no more difficult to synthesize billions of copies of a desired structure than it is to create a single copy; this is potentially a very powerful tool. Finally, the structures are easily controlled because of the programmability of the scaffolding material—DNA. Using DNA, we can control of the number and size of nanoparticles linked, the distance between

nanoparticles, the dimensionality of the structures, and the flexibility of the structures. Au nanoparticles were chosen as a model system due to the homogeneity of size and shape and their easy manipulation in a single solvent with straightforward chemistry. However, it is important to note that the protocol is general and can be extended to several other systems, such as semiconductor nanoparticles.

Two previous papers from our group have presented the synthesis of dimers and trimers of Au particles connected with DNA [15,16]. In these papers, complementary conjugates (particles attached to ssDNAs of complementary sequences) were combined to form dimers and trimers by DNA hybridization. Although a 1:1 Au:DNA ratio was used to produce particles bearing just one ssDNA, the binding of the ssDNA to the particle is a statistical process and the final number of ssDNAs per particle was not homogeneous. Usually, free particles, dimers and trimers were present in a final mixture if dimers were mixed, for example, which had to be purified afterwards. While this approach succeeded in generating small groupings of nanoparticles, it could not be extended to more complex systems. In addition, the low yield achieved (< 30%) for the generated structures was a limiting factor for the system characterization.

Here, we have used highly purified Au nanoparticle/DNA conjugates, i.e., particles bearing a specific number of ssDNA (1-5) [20] as building blocks to form dimers and trimers. This approach has produced the target structure in much higher yield and it has allowed us better control of the system, and improved understanding of the ssDNA attachment to the particle. Several issues have now been addressed, and the techniques developed will improve all future related research. By using gel electrophoresis, we could study the mobility of Au/DNA hybrid materials, pointing out the critical role of the surface charge of the particles. Besides dimers and trimers, intermediate building blocks could be also identified in the gel, such as dimers of particles bearing one extra ssDNA. The high yield in the final structures has allowed us to conduct better characterization by Transmission Electron Microscopy (TEM) and to develop a computer program to generate pair distribution functions from TEM images.

Materials and Methods

Gold colloids with mean diameters of 5 and 10 nm were either synthesized by the citrate/tannic acid method [21] or purchased (Ted Pella). Typical size distributions were about 15%. Particles were coated with a phosphine ligand (bis(p-sulphonatophenyl)phenylphosphine dihydrate, dipotassium salt (Strem Chemicals) as described previously [16,20] and concentrated up to µM range. The phosphine coating gives a net negative charge on the particle surface, giving stability in high concentrations and in buffer conditions. PAGE purified thiol-modified ssDNAs with 50, 80 and 100 bases (b) [22] were purchased from Intregated DNA Technologies (unless otherwise mentioned, the abbreviation ssDNA will stand for thiolated ssDNA in this work).

The generation of discrete Au nanoparticle/DNA conjugates has been described previously [20]. Briefly, Au nanoparticles were mixed with ssDNA and incubated for 2 h in 0.5x TBE, 50 mM NaCl. Gel electrophoresis (3% agarose gel @ 5 V/cm, 0.5x TBE, 1-2 h) was used to separate the different conjugates (particles bearing from 1 to 5 ssDNAs), which appeared as well-defined bands in the gel; the reddish color of Au colloid easily allows band identification. Each band was then recovered from the gel using standard procedures [16]. In order to avoid misunderstanding and repetition, we adopt the following nomenclature: first conjugate corresponds to particles bearing one ssDNA, second conjugate to particles bearing two equal ssDNA and so on. The mean size of Au particles is either 5 or 10 nm (note that small variation from batch to batch was found) and the ssDNA length is 50b, 80b or 100b. In this way, the abbreviation 1/5nmAu/100bssDNA corresponds to 5 nm Au particles bearing 1 ssDNA of 100b in length. The first number, then, refers to the number of ssDNA attached to the particle.

Ferguson plots for free ssDNA, unconjugated Au particles and corresponding conjugates have been obtained for gel concentrations between 0.5 and 6%. Special care was taken during gel preparation in order to precisely determine the agarose concentration. As already mentioned, the reddish color of the Au colloid allows band identification of free particles and conjugates, while ssDNA bands were

visualized by staining the gel with GelStar® nucleic acid stain (BioWhittaker Molecular Applications). The center of the band was the reference to measure particle mobilities.

Dimers and trimers of nanoparticles were formed by mixing stoichiometric amounts of the corresponding building block conjugates. For dimers, the first conjugates with complementary ssDNAs are mixed in equimolar amounts (final concentration ~ 3 μM), and incubated overnight in 50 mM NaCl or 0.5x TBE to allow the DNA hybridization. A 3% agarose gel is used to confirm the dimer formation. A similar protocol is used to form trimers of nanoparticles, but a 2:1 ratio of first and second complementary conjugates is mixed.

TEM studies were performed in an FEI Tecnai 12 TEM—100kV, at the Electron Microscope Laboratory—UC Berkeley, Berkeley, CA. Formvar coated grids were first treated with bacitracin (Sigma) for 30s, 500μg/ml, and then Au nanoparticle grouping samples (100-500 nM) were dropped and wicked off after 30s. For pair distribution analysis, grids were also washed with water for 30s both after bacitracin coating and after gold sample coating. A computer program was developed to analyze a series of dimers. Digital TEM images were recorded on a low resolution digital camera (Gatan Model 780 Dual View Camera, 1300 x 1300 pixel); approximately 50 images were recorded per grid, per sample. Magnification and particle density on the grid (changed via sample concentration in grid preparation) were optimized to provide rapid and accurate analysis. These images were analysed using Image Pro Plus graphics analysis software (Media Cybernetics, Inc.). Particles were counted by the program, and lists of particle locations were recorded. These lists were then used as input for a Labview (National Instruments) program written to calculate pair distribution functions from the lists of particle locations. Distances were collected in 1 nm bins; bins were normalized according to area. Pair distribution functions were created for unconjugated 5 and 10 nm particles, 5-5 dimers and 10-10 dimers connected with 50b, 80b and 100b DNA.

Results

6

Electrophoretic mobility of Au nanoparticle/ssDNA Conjugates

Nanoparticle/ssDNA conjugates are versatile building blocks that can be used to generate complex nanosystems. While the physical properties are mainly determined by the particle itself, the binding and addressability attributes are given by the sequence of the ssDNA attached to it. The possibility of creating a library of conjugates, by combining different particles and ssDNA sequences is then a challenging and tempting task. To pursue this aim, we have explored the electrophoretic mobility of nanoparticles, ssDNA and their conjugates.

Gel electrophoresis is a simple, powerful and widespread tool in the characterization and purification of biological systems. The basic principle relies on the characteristic mobility of particles—such as colloids, DNA, proteins, and conjugates—in a porous matrix, or gel, under an electric field. The mobility (distance/(electric field x time)) depends on both size and charge of the particle [23]. In the case of the Au nanoparticle/DNA system studied in this work, agarose gels are the most appropriate medium, due to the characteristic pore size (> 50 nm) and chemical compatibility. A typical image of a 3% agarose gel of Au nanoparticle/DNA conjugates is presented in fig.1a. The binding of each ssDNA to a nanoparticle decreases the particle mobility in a discrete way, making it possible to isolate highly purified samples of specific conjugates from the gel.

Although the mechanisms for particle motion through gels are complex, we can still derive insightful information about conjugates from gel electrophoresis. Ferguson plots, where the logarithm of mobility is plotted against gel percentage [24,25], provide information about the interplay between particle size and charge. For low gel concentrations (< 1%) the charge of the particle is the determining factor of its mobility, while for higher gel concentrations (> 3%), the particle size is the dominant factor. A typical plot of our system is given in fig. 1b. The Ferguson plot originates in the free volume model of gel electrophoresis, where the mobility of a particle is proportional to the fractional free volume in a gel. The fractional free volume decreases exponentially with increasing gel percentage, hence the logarithmic scale [26]. For small particles such as our ssDNA, the free volume model is a good

description, and the plot is linear. For hard spheres, such as nanoparticles and conjugates, as well as proteins, this model usually does not apply very well, and the Ferguson plots are not linear [27]. The main reason is that this simple model does not account for the fact that not all of the free volume is accessible to hard particles that cannot deform [26]. The fact that both free particles and conjugates behave in a similar way, indicates that the electrophoretic mobility of the conjugates are mainly determined by the nanoparticle.

Ferguson plot analysis can also be used to derive the optimum gel concentration for the resolution of the species in a given sample [24]. This is easily applied in biological systems where the molecules have well-defined size and charge. Unfortunately, this is not the case for nanoparticle samples, where both size and charge distributions are always present. Increasing the gel percentage and using more stringent conditions does not usually improve resolution due to the spreading of the bands. A similar effect was also found when we ran the gel for longer times, and in fact the resolution is more or less already determined after one hour in our system.

Another interesting characteristic related to electrophoretic mobility of Au/DNA conjugates studied for this work is that they migrate more slowly through gels than DNA or Au particles alone. This was not predicted beforehand, since the attachment of each ssDNA to the particle adds both size and charge to the system. The Au nanoparticles are coated by phosphine molecules and are therefore highly negatively charged. In this case, when a ssDNA is attached to the particle, the increase in size (volume) seems to be more important than the increase in charge and the overall conjugate has a slower mobility. This is not the case in another system that we are also studying [28,29]—silica-coated semiconductor nanocrystals, where the binding of ssDNA increases the mobility of the particles. The main reason for the opposite behavior is the different charge/size ratio of these systems. Different from the Au case, the silica-coated nanocrystals are almost neutral particles, and adding ssDNA gives negative charge to the particles. In this case, the particles migrate faster since the increase in charge is more pronounced than the increase in size.

The results obtained from the Ferguson plots and for different nanoparticle/DNA systems suggest that the surface charge on the particles is a critical parameter. By varying it, we may invert the band positions of particles and conjugates in the gel and the determining factor for the conjugate mobility. This is a very interesting property of the system, and it may be exploited, for example, to improve the resolution in the band separation of a desired conjugate. In the future, theoretical models based on charge/size ratio of particles and conjugates should allow us to predict the band position. The best resolution may also be achieved by optimizing the conditions (particle charge and gel percentage) for each system.

Nanoparticle groupings

Nanoparticle groupings are formed by interconnection of particles by a linker. DNA is one of the best linker candidates due to its remarkable properties such as specificity, recognition and programmability. By programming the ssDNA sequence on a particle's surface, one can specifically address the nanoparticle to a binding site.

We have used stoichiometric amounts of purified conjugates to generate small groupings of particles. These groupings were characterized using gel electrophoresis as well as TEM. It should be noted that UV/Vis spectroscopy is not a useful characterization technique for these groupings, since the gold particles connected with DNA are not close enough to produce a significant shift in the plasmon peak of the gold. Figure 2 shows the typical procedure for obtaining homodimers of 5 nm particles using 1/5nm/100bssDNA complementary conjugates. The first gel (fig. 2a) shows the bands corresponding to discrete conjugates of 5nmAu/100bssDNA (**A**). Each conjugate is then recovered from the gel; the typical yield being up to 30% for the most intense band. The conjugation yield can be adjusted to some extent by changing the Au/DNA ratio (increasing the DNA amount increases the higher order conjugate yield). In parallel, the same procedure is performed using 5 nm Au particles and complementary 100bssDNA (**A'**). The dimers are generated by mixing equimolar amounts of **A** and **A'** first conjugates

and incubated overnight. Figure 2b shows the final result: the first three lanes correspond to the reference samples, i.e., 5 nm Au particles, 1/5nm/100bssDNA (**A**) and complementary 1/5nm/100bssDNA (**A'**), and the fourth lane is the dimer sample. The dimer band can be easily identified in the fourth lane, as a retarded band, and it corresponds to more than 80% of the species in the sample. The slower mobility of dimers related to the former conjugates is explained by their larger size (sieving effect).

Extending this procedure to heterodimers of 5 and 10 nm particles (5/10) and homodimers of 10 nm particles (10/10) is straightforward. Figure 3 shows the resulting gel and the TEM images are presented in fig. 4. The first four lanes are the reference samples, and the following three lanes correspond to the 5/5, 5/10 and 10/10 dimers (left to the right). As expected, the dimer mobility depends on particle sizes. The other bands found in lanes 5-7 correspond to uncombined conjugates.

This methodology can also be easily extended to form more complex structures, such as trimers. In this case, the intermediary structures were also probed, such as dimers of particles bearing one extra ssDNA (dimer building block). This is important information for determining the usefulness of electrophoresis in this kind of study. Two different heterotrimers were built: 5/10/5 and 10/5/10. The first four lanes in the gel of fig. 5a are the references: 5 nm, 10 nm, 1/5nm/100bssDNA and 2/10nm/100bssDNA. Lanes 5-7 correspond to the combination of 1/5nm/100bssDNA and 2/10nm/100bssDNA in different ratios: 1:1, 2:1 and 5:1. The combination of the conjugates in a 1:1 ratio (lane 5) leads to appearance of a more retarded band, corresponding to the 5/10 dimer building block. Doubling the amount of 1/5nm/100bssDNA increases the intensity of this retarded band. Finally, using a 5:1 ratio, an additional retarded band is visible, corresponding to the trimer 5/10/5. It is worth pointing out that in this experiment the 5/10 dimer building block and the 5/10/5 trimer are not well separated, probably due to the small difference in the final structure size. On the other hand, the last lane corresponds to the 10/5/10 trimer, and we can see that its separation from the 10/5 dimer building block is clearer, due to a greater difference in size (a larger particle, 10 nm instead of 5 nm, is

added to the corresponding dimer building block). Figure 5b shows the TEM image of the 10/5/10 trimers. Although we cannot yet fully explain the reasons for the incomplete hybridization of the conjugates, the fact that we are dealing initially with purified samples is a prerequisite to overcoming this issue. Possible reasons could be related to the annealing process, ssDNA angle distribution and purification process.

Due to the improvement in the methodology and control of the system, we could then improve the TEM analysis to get information about the conformation of the final structure. Quantitative data can be extracted from the TEM images by the construction of pair distribution functions, where the distances between all pairs of particles in any given image were measured, binned according to distance, and then plotted. Here we present the results for 5/5 and 10/10 dimers as a function of DNA length (50, 80, and 100b). The extension of this methodology to other structures, such as heterodimers and trimers is underway [30]. Figure 6 shows the pair distribution functions for unconjugated 5 and 10 nm particles (a and b) and the dimers (c-h), where several common features can be seen in all plots. First, for all the cases (a-h), there is a peak at the diameter of the particles. This corresponds to the distance between the centers of aggregated particles; all grids show a small degree of aggregation due to the intrinsic difficulty of uniform spreading of the particles on a TEM grid. Second, a constant background shows up for larger distances due to the statistical spreading of particles on the grid. However, on the dimer plots (fig. 6c-h) an additional feature appears which shifts to larger distances as a function of DNA length, corresponding to the lengths of the dimers. Consider the case of 5/5 100b DNA dimers (fig. 6g): the expected interparticle distance can vary from 41 nm down to 27 nm due to the floppiness of the 5'-end thiol linkers (the 100b DNA length is approximately 34 nm, the linkers are roughly 1 nm each). Note that the persistence length for hybridized DNA is about 50 nm [23], so that 100b is a nearly rigid molecule. Looking at fig.6, all the cases show a peak in the range of possible dimer distances. Statistical analysis of the functions can be explored to evaluate quantitatively the structure populations and will be presented in an upcoming paper.

Concluding remarks

We have shown that Au nanoparticle/DNA conjugates are important building units for forming more complex nanoparticle groupings. Compared to previous work [15,16], the use of the purified conjugates has given much more control and understanding of the system. In particular, the electrophoretic mobility studies of particle/DNA hybrids have shown that particle properties dominate the mobility and that dimers, trimers, and intermediate building blocks could be identified in the gel. TEM analysis was extended by generating pair distribution functions from the images. This was applied to dimers of particles linked by different DNA lengths, pointing out the dependence of interparticle distance on DNA length.

The improvement in our ability to make and characterize Au nanoparticle/DNA structures suggests several routes for future work. One of the current challenges is the generation of discrete structures formed by more than two or three nanoparticles, and the use of conjugates makes it more realistic to pursue this. Towards this goal, additional mobility studies are underway [31] as well as the extension of the pair distribution function analysis for systems other than dimers; this will allow better evaluation of complex structures.

As a remark, the development of new isolation and characterization tools for nanoparticle/DNA structures must be continued. In particular, it will not be possible to isolate or probe large structures by gel electrophoresis, due to the finite gel pore size. Computer programs to analyze TEM images, such as the one presented here, are good ways to probe such structures. Techniques such as ultracentrifugation and Dynamic Light Scattering (DLS) may also give important information. A further possibility for flat structures is to image with Atomic Force Microscopy, targeting not only the particles but also the DNA linker.

The combination of different conjugates in different proportions can lead to the formation of a great variety of nanoparticle assemblies, from two (dimers) to numerous particles interconnected in a

particular way. The methodology is general and can be extended to other kinds of systems (nanoparticles and biomolecules), providing a vast library of building blocks. We expect that this will allow us in the near future to study the evolution of properties (optical, electrical) as a function of the number and distribution of interconnected nanoparticles in the same way that we now study the properties of assemblies of atoms.

References

[1] Michalet, X.; Pinaud, F.; Lacoste, T.D.; Dahan, M.; Bruchez, M.P.; Alivisatos, A.P.; Weiss, S. *Single Mol.* **2001**, *2*, 261.

[2] Storhoff, J.J.; Mirkin, C.A. *Chem Rev.* **1999**, *99*, 1849.

[3] Bruchez, M.; Moronne, M.; Gin, P.; Weiss, S.; Alvisatos, A.P. *Science* **1998**, *281*, 2013.

[4] Chan, W.C.W.; Nie, S. *Science* **1998**, *281*, 2016.

[5] Rosenthal, S.J.; Tomlinson, I.; Adkins, E.; Schroeter, S.; Adams, S.; Swafford, L.; McBride, J.; Wang, Y.; DeFelice, L.J.; Blakely, R.D. *J. Am. Chem. Soc.* **2002**, *124*, 4586.

[6] Taylor, J.R.; Fang, M.M.; Nie, S.M. *Anal. Chem.* **2000**, *72*, 1979.

[7] Han, M.Y.; Gan, X.H.; Su, J.Z.; Nie, S. *Nature Biotech.* **2001**, *19*, 631.

[8] Mattoussi, H.; Mauro, J.M.; Goldman, E.R.; Anderson, G.P.; Sundar, V.C.; Mikulec, F.W.; Bawendi, M.G. *J. Am. Chem. Soc.* **2000**, *122*, 12142.

[9] Gerion, D.; Parak, W.J.; Williams, S.C.; Zanchet, D.; Micheel, C.M.; Alivisatos, A.P. *J. Am. Chem. Soc.* **2002**, *124*, 7070.

[10] Parak, W.J.; Boudreau, R.; LeGros, M.A.; Gerion, D.; Zanchet, D.; Micheel, C.M.; Williams, S.C.; Alivisatos, A.P.; Larabell, C.A. *Adv. Mater.* **2002**, *14*, 882.

[11] Taton, T.A.; Mirkin, C.A.; Letsinger, R.L. *Science* **2000**, *289*, 1757.

[12] Reynolds, R.A.; Mirkin, C.A.; Letsinger, R.L. *J. Am. Chem. Soc* **2000**, 122, 3795.

[13] Whaley, S.R.; English, D.S.; Hu, E.L.; Barbara, P.F.; Belcher, A.M. *Nature* **2000**, *405*, 665.

[14] Mirkin, C.A.; Letsinger, R.L.; Mucic, R.C., Storhoff, J.J. *Nature* **1996**, *382*, 607-609.

[15] Alivisatos, A.P.; Johnsson, K.P.; Peng, X.; Wilson, T.E.; Loweth, C.J.; Bruchez, M.P.; Schultz, P.G. *Nature* **1996**, *382*, 609.

[16] Loweth, C.J.; Caldwell, W.B.; Peng, X.; Alvisatos, A.P.; Schultz, P.G. *Angew. Chem., Int. Ed.* **1999**, *12*, 1808.

[17] Connolly, S.; Fitzmaurice, D. *Adv. Mater.* **1999**, *11*, 1202.

[18] Shenton, W.; Davis, S.A.; Mann, S. *Adv. Mater.* **1999**, *11*, 449.

[19] Park, S.J.; Lazarides, A.A.; Mirkin, C.A.; Letsinger R.L. *Angew. Chem. Int. Ed.* **2001**, *40*, 2909.

[20] Zanchet, D.; Micheel, C.M.; Parak, W.J.; Gerion, D.; Alivisatos; A.P. *Nano Lett.* **2001**, *1*, 32.

[21] Handley, D.A. In *Colloidal gold: principles, methods and applications*; Hayat, M.A. Ed.; v.1; Academic Press: San Diego; pp 13-32, 1989.

[22]   ssDNA   sequences: 50b: 5'-XGCAGTAACGCTATGTGACCGAGAAGGATTCGCATTTGTAGTCTTGAGCCC-3';   80b: 5'-XGCAGTAACGCTATGTGACCGAGAAGGATTCGCATTTGTAGTCTTGAGCCCGCACGAAACC TGGACACCCCTAAGCAACTC-3';   100b: 5'-XGCAGTAACGCTATGTGACCGAGAAGGATTCGCATTTGTAGTCTTGAGCCCGCACGAAACC TGGACACCCCTAAGCAACTCCGTATCAGATGGGAACAGCA-3'; where X = 5'-thiol modifier.

[23] Noolandi, J. In *Advances in Electrophoresis*; A. Chrambach Ed.; v.5; VCH: Weinheim; pp 2-57, 1998.

[24] Ferguson, K. A. *Metabolism* **1964**, *13*, 985-1002.

[25] Slater, G.W.; Desruisseaux, C.; Hubert, S.J., Mercier, J.-F.; Labrie, J.; Boileau, J.; Tessier, F.; Pepin, M. *Electrophoresis* **2000**, *21*, 3873-3887.

[26] Slater, G.W.; Guo, H.L. *Electrophoresis* **1996**, *17*, 977-988.

[27] Tietz, D.; Chrambach, A. *Anal. Biochem.* **1987**, *161*, 395-411.

[28] Gerion, D.; Pinaud, F.; Williams, S.C.; Parak, W.J.; Zanchet, D.; Weiss, S.; Alivisatos, A.P *J. Phys. Chem. B.* **2001**, *105*, 8861.

[29] Parak, W.J.; Gerion, D.; Zanchet, D.; Woerz, A.S.; Pellegrino, T.; Micheel, C.; Williams, S.C.; Seitz, M.; Bruehl, R.E.; Bryant, Z.; Bustamante, C.; Bertozzi, C.R.; Alivisatos, A.P. *Chem. Mater.***2002**, *14*, 2113.

[30] Micheel, C.M. et al. *in preparation.*

[31] Parak, W.J. et al. *in preparation.*

Figure captions

Figure 1. (a) 3% agarose gel showing the 10nm/80bssDNA conjugates. Each band corresponds to particles bearing a well-defined number of ssDNAs; (b) Ferguson plot of 80bssDNA, 10 nm Au particles, and 1/10nm/80bssDNA.

Figure 2. (a) 3% agarose gel showing the 5nm/100bssDNA conjugates. To form 5/5 dimers, the first conjugate is collected (dashed square), mixed with an equimolar amount of a complementary conjugate (obtained by identical procedure), and incubated overnight in 50mM NaCl. (b) 3% agarose gel showing the dimer formation; the first three lanes (left to the right) are the references: 5 nm, 1/5nm/100bssDNA, complementary 1/5nm/100bssDNA and the last one is the dimer sample. The dimer band is retarded compared to the 1/5nm/100bssDNA due to the sieving effect.

Figure 3. Formation of different dimers: 5/5, 5/10 and 10/10. From left to the right: reference lanes, 5 nm, 10 nm, 1/5nm/100bssDNA, 1/10nm/100bssDNA; dimer lanes, 5/5, 5/10, 10/10. The dimer electrophoretic mobilities also decrease for larger particle size.

Figure 4. TEM images of the dimer bands, from the left to the right: 5/5, 5/10, 10/10. The scale bar is 100 nm.

Figure 5. (a) Trimer and dimer building blocks. Reference lanes (1)-(4) correspond to 5 nm, 10 nm, 1/5nm/100bssDNA and 2/10nm/100bssDNA. Lanes (5)-(7) correspond to the 5/10/5 trimer formation: (5) 1:1 mixture of 1/5nm/100bssDNA and 2/10nm/100bssDNA, (6) 2:1 ratio and (7) 5:1 ratio. The

addition of 1/5nm/100bssDNA to the 2/10nm/100bssDNA leads to the formation of the corresponding dimer building block (5/10 dimer with an extra ssDNA). Increasing the 1/5nm/100bssDNA ratio generated the trimer 5/10/5. Lane (8) corresponds to the 10/5/10 trimer and related building units; (b) TEM image of 10/5/10 trimers; scale bar 100nm.

Figure 6. Pair distribution functions of (a) 5 nm particles, (b) 10 nm particles (c) 5/5 dimers linked by 50b DNA, (d) 10/10 dimers linked by 50b DNA, (e) 5/5 dimers linked by 80b DNA, (f) 10/10 dimers linked by 80b DNA, (g) 5/5 dimers linked by 100b DNA, and (h) 10/10 dimers linked by 100b DNA. Note the clear evolution of the third peak of (c-g) as a function of DNA length; this corresponds to the interparticle distance in the corresponding dimers. The arrows for dimer distributions highlight the calculated maximum length of the dimers.
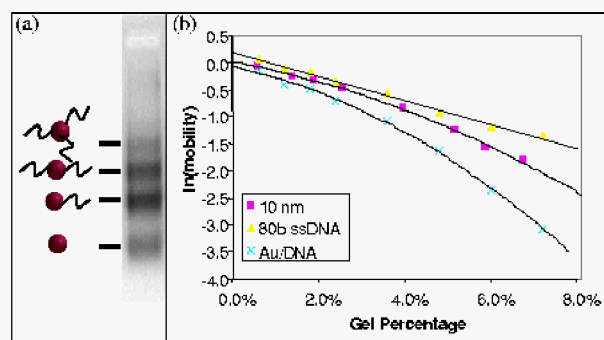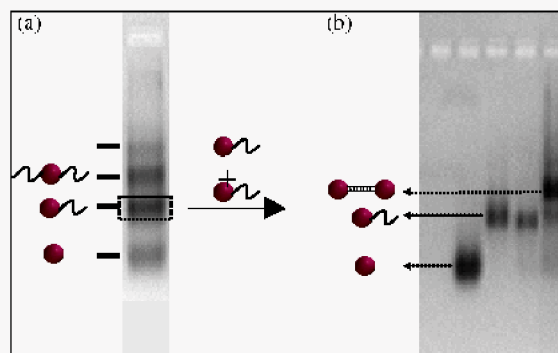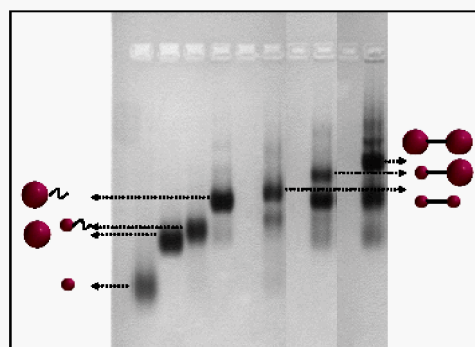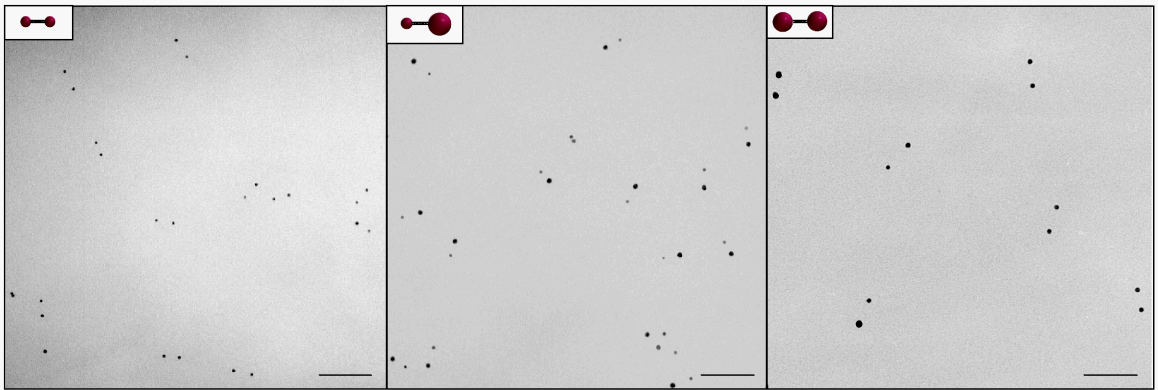
Fig.1

Fig. 2

Fig. 3

Fig. 4

Fig. 5

Fig. 6